JPET Fast Forward. Published on July 26, 2013 as DOI: 10.1124/jpet.113.203299
This article has not been copyedited and formatted. The final version may differ from this version.

Involvement of Wee1 in the circadian rhythm dependent intestinal damage induced by docetaxel

Yuri Obi-Ioka, Kentaro Ushijima, Mikio Kusama, Eiko Ishikawa-Kobayashi, and Akio Fujimura

Division of Clinical Pharmacology, Department of Pharmacology (Y.O-I., K.U., E.I-K., A.F.), and Department of Dentistry, Oral and Maxillofacial Surgery (Y.O-I., M.K.), Jichi Medical University

a) Running title: Wee1 and docetaxel chronotoxicity

b) Corresponding author: Akio Fujimura. MD. PhD

Division of Clinical Pharmacology, Department of Pharmacology, School of Medicine, Jichi Medical University, Tochigi 329-0498, Japan

Tel: +81 285 58 7387, Fax: +81 285 44 7562, E-mail: akiofuji@jichi.ac.jp

c) Number of text pages: 25

Number of tables: 2

Number of figures: 7

Number of references: 27

Abstract: 257 words

Introduction: 404 words

Discussion: 752 words

d) Abbreviations: cyclin-dependent kinase1, CDK1; hours after light on, HALO

e) Recommended section: Toxicology

ABSTRACT

Docetaxel, a semi-synthetic taxane, is effective for the treatment of some solid cancers; however, docetaxel-induced intestinal damage leads to poor prognosis in some patients. Although such adverse effects have been reported to depend on the dosing-time of docetaxel, the mechanisms involved remain unclear. Wee1 expression is controlled by the clock gene complex, *clock/bmal1* and contributes to cell cycle progression. The present study was undertaken to evaluate the potential role of Wee1 in the circadian rhythm dependent profile of docetaxel. Male mice were maintained under a 12-hr light/dark cycle. Intestinal damage after repeated dosing of docetaxel (20 mg/kg) for 3 weeks was more severe at 14HALO than at 2HALO (hours after light on). The intestinal protein expressions of Wee1, phosphorylated CDK1, and cleaved Caspase-3 were higher in the 14HALO group than in the 2HALO group, while that of survivin was lower in the 14HALO group. Thus, it is speculated that elevated Wee1 expression more inhibited CDK1 activity by phosphorylation, which in turn caused the lower expression of survivin and consequently more activated Caspase-3 in the 14HALO group. There were no significant differences in plasma docetaxel concentrations between the 2 and 14HALO groups. Bindings of CLOCK and BMAL1 to the E-box regions at the *wee1* gene promoter were not altered by docetaxel treatment at 2 and 14HALO. These findings suggest that Wee1 is directly or indirectly involved in the mechanism of the circadian rhythm dependent changes in docetaxel-induced intestinal damage. However, the mechanism for a circadian rhythm dependent change in intestinal Wee1 expression by docetaxel remains to be determined.

INTRODUCTION

Docetaxel {(-)-(1S,2S,3R,4S,5R,7S,8S,10R,13S)-4-Acetoxy-2-benzoyloxy-5,20-epoxy-1,7,10-trihydroxy-9-oxotax-11-ene-13-yl(2R,3S)-3-tert-butoxycarbonylamino-2-hydroxy-3-phenylpropionate trihydrate} is a semi-synthetic taxane derived from the needles of the European yew (Taxus baccata). This agent binds to tubulin, leading to its polymerization, promotes microtubule assembly, and inhibits tubulin depolymerization (Pellegrini and Budman, 2005). The disruption of microtubules causes cell arrest at the G2-M phase of the cell cycle, and subsequently leads to cell death by apoptosis or necrosis. Docetaxel causes cell death mainly by mitotic catastrophe (Morse, 2005; Fabbri, 2008), which is an aberrant form of mitosis and induces cell death by defects in mitosis (Roninson, 2001). Mitotic catastrophe, a process preceding apoptosis- or necrosis- induced cell death (Vakifahmetoglu, 2008), is controlled by numerous molecular factors such as cell-cycle-specific kinases [including cyclin-dependent kinase1 (CDK1), polo-like kinases and aurora kinases], cell-cycle checkpoint proteins, survivin, p53, caspases and members of the Bcl-2 family (Castedo, 2004).

Many physiological functions show circadian rhythms that are regulated by a biological clock system as follows (Mohawk, 2012); 1) A central clock in the suprachiasmatic nucleus influences peripheral clocks through hormonal and neural signals. 2) Individual peripheral tissues also have their own clock system, and express a self-sustained circadian oscillation. 3) The clock system contains the following clock genes; *clock, bmal1*, *per*1-3 and *cry*1-2. Clock and Bmal1, the basic helix-loop-helix transcriptional activators, are positive regulators of the clock system, while Per1-3 and Cry1-2 are negative.

Although myelosuppression is generally a major dose-limiting toxicity for cancer chemotherapies, prophylactic use of granulocyte-colony-stimulating factors and improved transplantation procedures ameliorate this adverse effect in many patients. On the other hand, non-hematological toxic effects such as mucositis have now become the dose-limiting factor.

A recent study showed that cell cycle progression is under the influence of the circadian clock through the clock-controlled gene, *wee*1 (Gerard and Goldbeter, 2012). Wee1 protein is a tyrosine kinase that selectively phosphorylates the Tyr15 residue of CDK1 and inactivates its activity, (Chow and Poon, 2012; Magnussen, 2012), leading to G2/M arrest.

The toxicity and efficacy of anti-cancer drugs have been shown to be improved by their optimal dosing-time (Innominato, 2010). A previous animal study showed that the frequency of docetaxel-induced severe damage in the intestinal mucosa was greater after dosing at an active phase than at an inactive phase in mice (Tampellini, 1998). However, the underlying mechanism(s) of such dosing-time dependent intestinal toxicity remains to be determined. This study was undertaken to evaluate the potential role of Wee1 in the chronotoxicological profile of docetaxel in mice.

MATERIALS and METHODS

Animals and synchronization

Five-week-old, male Balb/c mice (SLC, Hamamatsu, Japan) were maintained under a 12-hr light/dark cycle in a temperature-controlled room (23 ± 1 ^{o}C) with food and water ad libitum. All mice were synchronized for more than two weeks before the initiation of the experiment. Time was expressed as hours after light on (HALO); 2, 6 and 10 HALO were during the light period when mice were commonly inactive, while 14, 18 and 22 HALO corresponded to the

dark period when animals were commonly active. The experiment was approved by the Ethics Committee of Jichi Medical University (No. 12022, Tochigi, Japan) and performed in accordance with the Use and Care of Experimental Animals Committee of Jichi Medical University.

Preparation of the dosing solution

Docetaxel (Taxotere®) was kindly supplied by Sanofi-Aventis (Tokyo, Japan). The drug was injected intraperitoneally. Docetaxel was dissolved in a solution to store 10 mg/ml, and further diluted with saline just before each injection. The volume of the drug solution given to mice each time was 0.02 ml/g.

Evaluation of intestinal apoptosis

Docetaxel (0, 10, 20, 30, 40, 60 and 80 mg/kg/week) was given once a week for 3 weeks for mice. Because more than 30 mg/kg/week of the drug caused body weight loss in mice (Supplemental Fig. 1), 20 mg/kg/week of docetaxel was judged to be the maximum non-toxic dose.

Docetaxel (20 mg/kg/week) was given to mice once a week for 3 weeks at one of the following different points (2, 10, 14 or 22 HALO). Seventy two hrs after the final dosing of the agent, the intestinal mucosa of the small intestine (proximal 8 cm) was removed, fixed in 20N Mildform® solution (containing 8% formaldehyde in a buffered solution, Wako Pure Chemical Industries, Osaka, Japan), and embedded in paraffin blocks, and sections of 5 μm were put on glass slides. Apoptosis was detected using the terminal deoxynucleotidyl transferase-mediated dUTP nick end-labeling (TUNEL) method (Noda, 1998) using the Apop Tag peroxidase in situ apoptosis detection kit (S7100, Chemicon, Billerica, MA). Specimens

were dewaxed and immersed in phosphate-buffered saline for 5 min at room temperature, then incubated with 20 μg/ml proteinase K for 15 min at room temperature, and quenched of endogenous peroxidase in 2% hydrogen peroxide in phosphate-buffered saline. Terminal deoxynucleotidyl transferase enzyme was applied directly onto the specimens, which were then incubated at 37°C for 1 hr. The reaction was terminated by transferring the slides to stop/wash buffer for 10 min at room temperature, and then specimens were covered with peroxidase-conjugated anti-digoxigenin antibody and incubated for 30 min at room temperature. Specimens were then soaked in staining buffer containing 0.05% diaminobenzidine to achieve color development. Finally, the specimens were counterstained by immersion in Mayer's Hematoxylin solutuion. Apoptotic cells were counted under a light microscope in a good longitudinal crypt section. Starting at the base of the crypt column, the TUNEL-positive cells were counted up to the 18th cell position in each crypt. One hundred crypt sections were scored in each animal, and a frequency of TUNEL-positive cells per crypt was calculated (Ijiri and Potten, 1983). Dosing-time dependent influence of docetaxel on intestinal apoptosis was also examined in female Balb/c mice.

Protein extraction, immunoprecipitation, and western blotting

Docetaxel (20 mg/kg) was given to mice once at 2 and 14 HALO. In a preliminary study, we measured an intestinal Wee1 protein expression level before and at 24, 48 and 72 hrs after dosing of 20 mg/kg docetaxel. Wee1 protein expression level time-dependently increased, reached to the highest at 48 hrs and returned to the base-line at 72 hrs after dosing. Therefore, the small intestine containing epithelial cells and smooth muscles was obtained 48 hrs after dosing of the agent.

A small intestinal sample was homogenized in lysis buffer [50 mM Tris-HCl (pH7.5), 150

mM NaCl, 0.1% Triton-X 100, 0.1% Nonidet P-40, 4 mM EDTA, 4 mM NaF, 0.1 mM Na_3VO_4, 0.1 mM phenylmethylsulfonyl fluoride, and protease and phosphatase inhibitor cocktails (Nacalai Tesque, Kyoto, Japan)] and incubated on ice for 30 min. Insoluble debris was pelleted and the protein concentration in the supernatant was determined using a BCA Protein Assay kit (Thermo Fisher Scientific, Rockford, IL).

For the analysis of Bax, cleaved Caspase-3, Wee1, survivin and β-actin, lysate samples containing 20 μg of total protein were separated by SDS-PAGE and transferred to a polyvinylidene difluoride membrane. The membrane was reacted with antibodies against Bax (1 μg/mL), Wee1 (1.5 μg/mL), surviving (1 μg/mL), β-actin (2 μg/mL) (Abcam, Cambridge, UK) or cleaved Caspase-3 (31 ng/mL) (Cell Signaling Technology, Denver, MA). For the analysis of CDK1 phosphorylation [p-CDK1 (Tyr 15)] and CDK1, intestine lysate (1.8 mg protein) was immunoprecipitated with an anti-CDK1 antibody (Santa Cruz Biotechnology, Santa Cruz, CA) at 4 ^{o}C overnight. Immunocomplexes were captured with protein A agarose (Roche Applied Science, Indianapolis, IN), and samples were allowed to mix at 4 ^{o}C for 2 hrs. Immunoprecipitates were washed and then separated by SDS-PAGE and transferred to a polyvinylidene difluoride membrane. Subsequently, the membrane was reacted with an anti p-CDK1 (Tyr 15) (2 μg/mL) or anti CDK1 (2 μg/mL) antibody (Santa Cruz). Specific antigen-antibody complexes were visualized using horseradish peroxidase-conjugated secondary antibodies and an ECL Plus detection kit (GE Healthcare, Buckinghamshire, UK).

RNA extraction and real-time PCR analysis

Docetaxel (20 mg/kg) was given to mice once at one of the following six different points (2, 6, 10, 14, 18 or 22 HALO), and the small intestine containing epithelial cells and smooth muscles was obtained 48 hrs after dosing of the agent. Intestinal total RNA was isolated using

an RNeasy Mini Kit (QIAGEN, Valencia, CA) and reverse transcription was performed using the PrimeScript® RT reagent kit (Takara Bio, Shiga, Japan) according to the manufacturer's instructions. Gene expression was analyzed by real-time quantitative PCR with the ABI Prism 7700 sequence detection system (Life Technologies, Carlsbad, CA). Specific primer sequences were described in Table 1. Each mRNA expression level of the target gene was normalized to the expression of GAPDH. Data were analyzed using the comparative threshold cycle method (Livak and Schmittgen, 2001).

Chromatin immunoprecipitation (ChIP) and real-time PCR analysis

Docetaxel (20 mg/kg) was given to mice once at 2 and 14 HALO, and the small intestine containing epithelial cells and smooth muscles was obtained 48 hrs after dosing of the agent. The intestine was fixed with 1% formaldehyde at room temperature for 15 minutes. The sample was homogenized, and cross-linked chromatin was sonicated on ice. ChIP was performed using Dynabeads Protein G (Invitrogen, Carlsbad, CA), and a fragmented chromatin was incubated with the antibody against CLOCK (Abcam) and BMAL1 (Novus Biologicals, Littleton, CO). DNA was purified and amplified using real-time PCR for the surrounding E-boxes in the promoter region of the *wee1* gene. The sequences of primers and probes for amplification were described in Table 2.

Plasma docetaxel concentrations

Docetaxel (20 mg/kg) was given to mice once at 2 and 14 HALO. Blood was collected 0.5, 1, 2, 4 and 8 hrs after the injection, and was centrifuged. Sample extraction was performed as described (Vergniol, 1992) with minor modifications. Plasma sample (150 µl) spiked with 10 µl of an internal standard solution (paclitaxel 5 mg/ml) was mixed with 250 ml of water. This

aqueous solution was loaded onto a C2 Bond Elute microcolumn (Varian, Harbor City, CA), which was preactivated with 1 ml of methanol and 1 ml of water. A wash step was performed using 1 ml water and 1 ml of 5% methanol. The cartridge was removed to another collection tube and the sample was eluted using 120 µl of methanol. The eluate was directly applied to HPLC analysis.

The HPLC system consisted of a liquid pump (PU-2080Plus, JASCO Co., Tokyo, Japan), a degasser (DG-2080-54, JASCO), an autosampler (AS-2059Plus, JASCO) and a UV detector (UV-2070Plus, JASCO). Control of the HPLC system and data collection was performed by ChromNAV (JASCO). The column was a Mightysil RP-18 (4.6 × 250 mm, 5µm, KANTO Chemical Co., Inc., Tokyo, Japan) fitted with a RP-18 guard column (4.6 × 5 mm, 5µm, KANTO Chemical). The mobile phase contained methanol and 0.3% orthophosphoric acid (73:27), its flow rate was 1.0 ml/min, and UV detection was employed at 225 nm. Calibration curves (using peak height ratios) were linear over the range 100-5000 ng/ml (r^2= 0.997). The coefficients of variation were 3.2 % (intra-day) and 5.7 % (inter-day).

Statistical analysis

Groups were compared by one-way or two-way ANOVA, and the difference between the two groups was analyzed by the Bonferroni-Dunn test. Daily rhythmicity was analyzed by the Cosinor method and one-way ANOVA. $P<0.05$ was considered to be significant.

RESULTS

Dosing-time dependent influence on docetaxel-induced apoptosis in the mouse intestine (Fig. 1)

Docetaxel (20 mg/kg) or vehicle was given once a week for 3 weeks to mice. At the end of the trial, apoptotic bodies in the intestine crypt significantly increased with docetaxel in the 2, 10 and 14 HALO groups. The variability in the docetaxel-treated 14 HALO group was significantly greater than that of the drug-treated 2 HALO group. In female mice, the docetaxel-induced intestinal apoptosis in the 14 HALO group was also significantly greater than that in the 2 HALO group (Supplemental Fig. 2).

Dosing-time dependent influence of docetaxel on Bax, cleaved Caspase-3, Wee1, CDK1 phosphorylation, and survivin in the mouse intestine (Fig. 2-3)

To evaluate the potential molecular mechanism involved in the chronotoxicological profile of docetaxel, the expressions of Bax, cleaved Caspase-3, Wee1, CDK1, and survivin were determined 48 hrs after repeated dosing of the agent at 2 and 14 HALO.

Bax expression was significantly elevated by docetaxel in the 2 HALO group, but not in the 14 HALO group. On the other hand, cleaved Caspase-3 expression was significantly elevated by docetaxel in the 14 HALO group, but not in the 2 HALO group.

The expressions of Wee1 and phosphorylated CKD1 were significantly elevated after dosing of docetaxel at 14 HALO, but not at 2 HALO. In addition, docetaxel significantly reduced survivin expression in the 14 HALO group, but not 2 HALO group. The survivin expression level in the docetaxel-treated 14 HALO group was significantly smaller than that in the drug-treated 2 HALO group.

Dosing-time dependent influence of docetaxel on Wee1 and clock gene mRNA expressions in the mouse intestine (Fig. 4)

The expression of Wee1 mRNA in the vehicle-treated group showed a significant daily

rhythm with a peak at 14 HALO ($p<0.01$ by Cosinor and $p<0.01$ by ANOVA). Docetaxel significantly elevated its expression after dosing at 14 HALO, and its expression level in the docetaxel-treated 14 HALO group was greater than that in the drug-treated 2 HALO group.

Bmal1 mRNA expression in the vehicle-treated group also showed a significant daily rhythm with a peak at 22 HALO ($p<0.01$ by Cosinor and $p<0.01$ by ANOVA), while Clock mRNA expression did not. Docetaxel did not change the expressions of these clock genes.

ChIP analysis at the *wee1* gene promoter in the mouse intestine (Fig. 5)

ChIP analysis at the *wee1* gene promoter in the mouse intestine was performed 48 hrs after dosing of docetaxel. The bindings of CLOCK and BMAL1 to E-box regions were not altered by the docetaxel treatment at 2 and 14 HALO.

Chronopharmacokinetic study of docetaxel (Fig. 6)

Plasma docetaxel concentrations were measured after dosing of the agent (20 mg/kg) at 2 and 14 HALO. Plasma drug concentrations were not detected at 8 hrs in both groups. There were no significant differences in plasma docetaxel concentrations between the 2 and 14 HALO groups at any sampling points.

Discussion

Docetaxel is effective in the treatment of some solid cancers such as breast, lung, ovarian, and prostate cancers, and improves the survival of these patients (Montero, 2005). However, mucositis is one of the dose-limiting toxic effects of docetaxel, and leads to poor prognosis in some patients (Ibrahim, 2000). Therefore, a safer regimen is needed to ameliorate this

drug-induced adverse effect. Chronotherapy is one of the approaches used to address this issue. The frequency of docetaxel-induced severe damage in the intestinal mucosa has been reported to be greater after dosing at an active phase than that at an inactive phase in mice (Tampellini, 1998). The present study also provided results to indicate that docetaxel-induced intestinal damage is greater during repeated dosing at an active phase in mice.

The mammalian cell cycle network is coupled to the circadian clock, *Clock/Bmal1*, through circadian variations in the Wee1 protein (Gerard and Goldbeter, 2012). A previous study using the small intestine in mice showed that the mRNA expressions of Bmal1 and Wee1 exhibited circadian variations with peaks at the late dark period and early dark period, respectively (Polidarova, 2009), which are similar to the present findings. In addition, this study showed for the first time that repeated treatment with docetaxel elevated Wee1 mRNA expression, especially at the early dark period (14 HALO).

Wee1 has been reported to inhibit CDK1 activity by phosphorylation (Chow and Poon, 2012; Magnussen, 2012), which in turn decreases survivin (Chen, 2013) and consequently activates Caspase-3 (Jones, 2010; Rubio, 2012). The phosphorylation of CDK1 and decrease in survivin are also involved in the mechanism of apoptosis via mitotic catastrophe (Castedo, 2008; Lamers, 2011). In this study, the following results were obtained after repeated dosing of docetaxel at 14 HALO; the intestinal protein expressions of Wee1 and phosphorylated CDK1 increased and that of survivin decreased. In addition, intestinal cleaved Caspase-3 expression was elevated in the 14 HALO group. However, these docetaxel-related changes were relatively small in the 2 HALO group. Based on these findings, the Wee1-CDK1-survivin-Caspase-3 pathway is thought to be involved in the mechanism of dosing-time dependent changes in docetaxel-induced intestinal damage (Fig. 7). Docetaxel has multiple anti-cancer mechanisms including the upregulation of Bax (Mhaidat, 2007; Ye,

2012). In this study, intestinal Bax expression was significantly elevated in the 2 HALO group after repeated dosing of docetaxel. Therefore, the Bax-related pathway may have been involved in the drug-induced intestinal damage observed in this study. However, this pathway may not play a major role in the dosing-time dependent intestinal damage induced by docetaxel.

Repeated dosing of docetaxel elevated the intestinal mRNA expression of Wee1, especially at 14 HALO, but did not change those of Bmal1 and Clock in this study. The transcription of *wee1* is directly regulated through the binding of Clock-Bmal1 heterodimers to E-box sequences in the promoter region (Matsuo, 2003). Therefore, to evaluate the potential mechanism, the dosing-time dependent influence of docetaxel on the binding of CLOCK and BMAL1 to the E-box regions at the *wee1* gene promoter was examined in 2 and 14HALO groups. Because the bindings of these proteins to E-box regions were not altered by repeated dosing of docetaxel at 2 and 14 HALO, such a mechanism may not be involved in the dosing-time dependent influence on intestinal Wee1 expression. Dosing-time has been reported to influence the blood concentrations of many drugs and consequently their effects or adverse effects (Lemmer, 2000). In this study, no significant differences were observed in plasma docetaxel concentrations between the 2 and 14 HALO groups. Therefore, chronopharmacokinetic differences may not be involved in the mechanism of the dosing-time dependent influence of docetaxel on intestinal Wee1 expression. Further study is needed to evaluate the mechanism(s) of this chronotoxicological event.

The present and previous (Montero, 2005) studies showed that docetaxel-induced intestinal damage was less severe after dosing of the agent during the light period than during the dark period in nocturnal rodents. In addition, the antitumor effect of docetaxel was also reported to be enhanced during repeated dosing at the light period (Montero, 2005). Our preliminary

study showed that the antitumor effect of docetaxel after dosing at 2 HALO was similar to that after dosing at 14 HALO (data not shown). Based on these findings in nocturnal rodents, we suggest that repeated dosing of docetaxel at night is a safer regimen for ameliorating drug-induced intestinal damage in human cancer patients. It is also anticipated that dosing at night may not diminish the antitumor effect of docetaxel. Clinical studies with cancer patients are needed to confirm these hypotheses.

Authorship Contributions

Participated in research design: Obi, Kusama, and Fujimura

Conducted experiments: Obi, Ushijima, and Ishikawa-Kobayashi

Contributed new reagents or analytic tools: Obi

Performed data analysis: Obi and Ushijima

Wrote or contributed to the writing of the manuscript: Ushijima, Kusama, and Fujimura

References

Castedo M, Perfettini JL, Roumier T, Andreau K, Medema R, and Kroemer G (2004) Cell death by mitotic catastrophe: a molecular definition. *Oncogene* **23**: 2825–2837.

Chen Y, Tsai YH, and Tseng SH (2013) Inhibition of cyclin-dependent kinase1-induced cell death in neuroblastoma cells through the microRNA-34a-MYCN-survivin pathway. *Surgery* **153**: 4-16.

Chow JPH and Poon RYC (2012) The CDK1 inhibitory kinase MYT1 in DNA damage checkpoint recovery. *Oncogene* (doi: 10.1038/onc.2012.504)

Fabbri F, Amadori D, Carloni S, Brigliadori G, Tesei A, Ulivi P, Rosetti M, Vannini I, Arienti C, Zoli W, and Silvestrini R (2008) Mitotic catastrophe and apoptosis induced by docetaxel in hormone-refractory prostate cancer cells. *J Cell Physiol* **217**: 494-501.

Gerard C and Goldbeter A (2012) Entrainment of the mammalian cell cycle by the circadian clock: Modeling two coupled cellular rhythms. *PLoS Comput Biol* **8**: e1002516.

Ibrahim NK, Sahin AA, Dubrow RA, Lynch PM, Boehnke-Michaud L, Valero V, Buzdar AU, and Hortobagyi GN (2000) Colitis associated with docetaxel-based chemotherapy in patients with metastatic breast cancer. *Lancet* **355**: 281-283.

Ijiri K and Potten CS (1983) Response of intestinal cells of differing topographical and hierarchical status to ten cytotoxic drugs and five sources of radiation. *Br J Cancer* **47**: 175-185

Innominato PF, Levi FA, and Bjarnason GA (2010) Chronotherapy and the molecular clock: clinical implications in oncology. *Adv Drug Deliv Rev* **62**: 979-1001

Jones MK, Padilla OR, and Zhu E (2010) Survivin is a key factor in the differential susceptibility of gastric endothelial and epithelial cells to alcohol-induced injury. *J Physiol*

Pharmacol **61**: 253-264.

Lamers F, van der Ploeg I, Schild L, Ebus ME, Koster J, Hansen BR, Koch T, Versteeg R, Caron HN, and Molenaar JJ (2011) Knockdown of survivin (BIRC5) causes apoptosis in neuroblastoma via mitotic catastrophe. *Endocr Relat Cancer* **18**: 657-668.

Lemmer B (2000) Relevance for chronopharmacology in practical medicine *Semin Perinatol* **24**: 280-290.

Livak KJ, and Schmittgen TD (2001) Analysis of relative gene expression data using real-time quantitative PCR and the 2(-Delta Delta C(T)) Method. *Methods* **25**: 402-408.

Magnussen GI, Holm R, Emilsen E, Rosnes AKR, Slipicevic A, and Florenes VA (2012) High expression of wee1 is associated with poor disease-free survival in malignant melanoma: potential for targeted therapy. *PLoS ONE* **7**: e38254.

Matsuo T, Yamaguchi S, Mitsui S, Emi A, Shimoda F, and Okamura H (2003) Control mechanism of the circadian clock for timing of cell division in vivo. *Science* **302**: 255-259.

Mhaidat NM, Wang Y, Kiejda KA, Zhang XD, and Hersey P (2007) Docetaxel-induced apoptosis in melanoma cells is dependent on activation of caspase-2. *Mol Cancer Ther* **6**: 752-761.

Mohawk JA, Green CB, and Takahashi JS (2012) Central and peripheral circadian clocks in mammals. *Annu Rev Neurosci* **35**: 445-462.

Montero A, Fossella F, Hortobagyi G, and Valeno V (2005) Docetaxel for treatment of solid tumours: a systematic review of clinical data. *Lancet Oncol* **6**: 229-239.

Morse DL, Gray H, Payne CM, and Gillies RJ (2005) Docetaxel induces cell death through mitotic catastrophe in human breast cancer cells. *Mol Cancer Ther* **4**: 1495-1504.

Noda T, Iwakiri R, Fujimoto K, Matsuo S, and Aw TY (1998) Programmed cell death induced by ischemia-reperfusion in rat intestinal mucosa. *Am J Physiol* **274**: G270-G276.

Pellegrini F and Budman DR (2005) Review: Tubulin function, action of antitubulin drugs, and new drug development. *Cancer Invest* **23**: 264-273.

Polidarova L, Sotak M, Sladek M, Pacha J, and Sumova A (2009) Temporal gradient in the clock gene and cell-cycle checkpoint kinase *WEE1* expression along the gut. *Chronobiol Int* **26**: 607-620.

Roninson IB, Broude EV, and Chang BD (2001) If not apoptosis, then what? Treatment-induced senescence and mitotic catastrophe in tumor cells. *Drug Resist Updat* **4**: 303-313.

Rubio N, Garcia-Segura LM, and Arevalo MA (2012) Survivin prevents apoptosis by binding caspase-3 in astrocytes infected with the BeAn strain of Theiler's murine encephalomyelitis virus. *J neurovirol* **18**: 354-363.

Tampellini M, Filipski E, Liu XH, Lemaigre G, Li XM, Vrignaud P, François E, Bissery MC, and Lévi F (1998) Docetaxel chronopharmacology in mice. *Cancer Res* **58**: 3896-3904.

Vakifahmetoglu H, Olsson M, and Zhivotovsky B (2008) Death through a tragedy: mitotic catastrophe. *Cell Death Differ* **15**: 1153–1162.

Ye QF, Zhang YC, Peng XQ, Long Z, Ming YZ, and He LY (2012) Silencing notch-1 induces apoptosis and increases the chemosensitivity of prostate cancer cells to docetaxel through Bcl-2 and Bax. *Oncol Lett* **3**: 879-884

Vergniol JC, Bruno R, Montay G, and Frydman A (1992) Determination of taxotere in human plasma by a semi-automated high-performance liquid chromatographic method. *J Chromatogr* **582**: 273-278

Footnotes

This study was supported by the Program for the Strategic Research Foundation at Private Universities 2011-2015 “Cooperative Basic and Clinical Research on Circadian Medicine” from the Ministry of Education, Culture, Sports, Science and Technology of Japan [A.F.], and by the Japan Research Foundation for Clinical Pharmacology [Y. O-I.]. This study was subsidized by the Japan Keirin Association through its promotion funds from Keirin Race [901811, 902006].

Figure Legends

Figure 1

Dosing-time dependent influence of docetaxel on apoptosis in the mouse intestine

□ vehicle, ■ docetaxel, Mean ± SE, n=7-8 in each,

** p< 0.01 vs. vehicle, ## p<0.01 vs. 2 HALO

Figure 2

Dosing-time dependent influence of docetaxel on apoptosis-related proteins in the mouse intestine

Representative images of western blot were shown in the top panel. The mean value of the vehicle group at 2 HALO was set to be 1.0.

□ vehicle, ■ docetaxel (DOC), Mean ± SE, n=6-7 in each,

* p<0.05 vs. vehicle

Figure 3

Dosing-time dependent influence of docetaxel on the G2-M cell cycle (Fig.3-1) and survivin (Fig.3-2) protein expressions in the mouse intestine

Representative images of western blot were shown in the top panel. The mean value of the vehicle group at 2 HALO was set to be 1.0.

□ vehicle, ■ docetaxel (DOC), Mean ± SE, n=6-7 in each in Fig.3-1, n=8 in each in Fig.3-2

* p< 0.05 vs. vehicle, ## p< 0.01 vs. 2 HALO

Figure 4

Relative mRNA expressions of Wee1 (Fig.4-1) and clock genes (Fig.4-2) in the mouse

intestine 48 hrs after dosing of docetaxel at 6 different time points

The mean value of the vehicle group at 2 HALO was set to be 1.0.

□ vehicle, ■docetaxel, Mean ± SE, n=5-7 in each in Fig.4-1, n=4 in each in Fig.4-2

** p< 0.01 vs. vehicle, ## p<0.01 vs. 2 HALO (Fig.4-1); # p<0.05 and ## p<0.01 vs. 22 HALO (Fig.4-2)

Figure 5

Chromatin immunoprecipitation (ChIP) analysis at the *wee1* gene promoter in the mouse intestine 48 hrs after dosing of docetaxel

Line (▬) of upper panel shows a schematic image of the target regions for PCR amplification in the ChIP analysis. Arrows represent the regions of the primer setting for amplification analysis. Cross-linked chromatin was expressed as the percentage of immunoprecipitated DNA fragments with regard to the input control.

□ vehicle, ■docetaxel, Mean ± SE, n=4-5 in each

Figure 6

Plasma docetaxel concentrations after dosing of the agent (20 mg/kg) at 2 HALO (◯) or 14 HALO (●) in mice

Mean ± SE, n=4 in each point

Figure 7

Schematic potential mechanism of the dosing-time dependent change in docetaxel-induced intestinal damage

JPET Fast Forward. Published on July 26, 2013 as DOI: 10.1124/jpet.113.203299
This article has not been copyedited and formatted. The final version may differ from this version.

Bold arrows indicate potential mechanistic pathway that docetaxel-induced intestinal damage was greater after dosing at 14 HALO than at 2 HALO.

JPET Fast Forward. Published on July 26, 2013 as DOI: 10.1124/jpet.113.203299
This article has not been copyedited and formatted. The final version may differ from this version.

Table 1 Sequences of primers for real-time PCR analysis

Gene symbol		Primer Sequence
Gapdh	Forward	5'-TGTGTCCGTCGTGGATCTGA-3'
	Reverse	5'-TTGCTGTTGAAGTCGCAGGAG-3'
Wee1	Forward	5'-GAAACAAGACCTGCCAAAAGAA-3'
	Reverse	5'-GCATCCATCTAACCT CTTCACAC-3'
Bmal1	Forward	5'-ACGACATAGGACACC TCGCAGA-3'
	Reverse	5'-CGGGTTCATGAAACTGAACCATC-3'
Clock	Forward	5'-AACCGTAGCAGGTTTATGGGAATG-3'
	Reverse	5'-TTGGTGTCCACACAATAGGCAAG-3'

JPET Fast Forward. Published on July 26, 2013 as DOI: 10.1124/jpet.113.203299
This article has not been copyedited and formatted. The final version may differ from this version.

Table 2 Sequences of primers and probes for ChIP analysis

Gene symbol		Primer Sequence
Per1-E-box1	Forward	5’-CAAAATCGCGTAGCTGGTT-3’
	Reverse	5’-CAAGTTCGTCCGCAAGTTC-3’
	Probe	5’-FAM-CTACGTCGCGCCCTCCCTGT-TAMRA-3’
Per1-E-box2	Forward	5’-AGTTTGGCTAGCGCACTCTC-3’
	Reverse	5’-CTCACAGCCAGACTTATCCG-3’
	Probe	5’-FAM-AGCCCGAATGCC TGACCTGC-TAMRA-3’

JPET Fast Forward. Published on July 26, 2013 as DOI: 10.1124/jpet.113.203299
This article has not been copyedited and formatted. The final version may differ from this version.

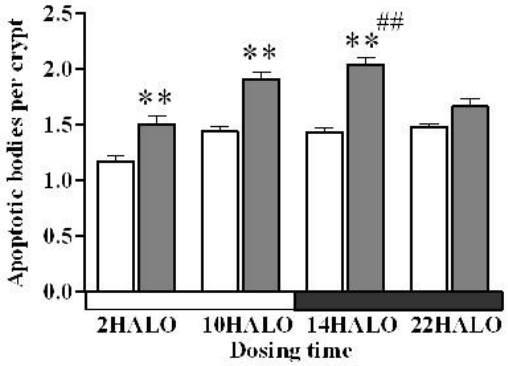

Fig. 1

JPET Fast Forward. Published on July 26, 2013 as DOI: 10.1124/jpet.113.203299
This article has not been copyedited and formatted. The final version may differ from this version.

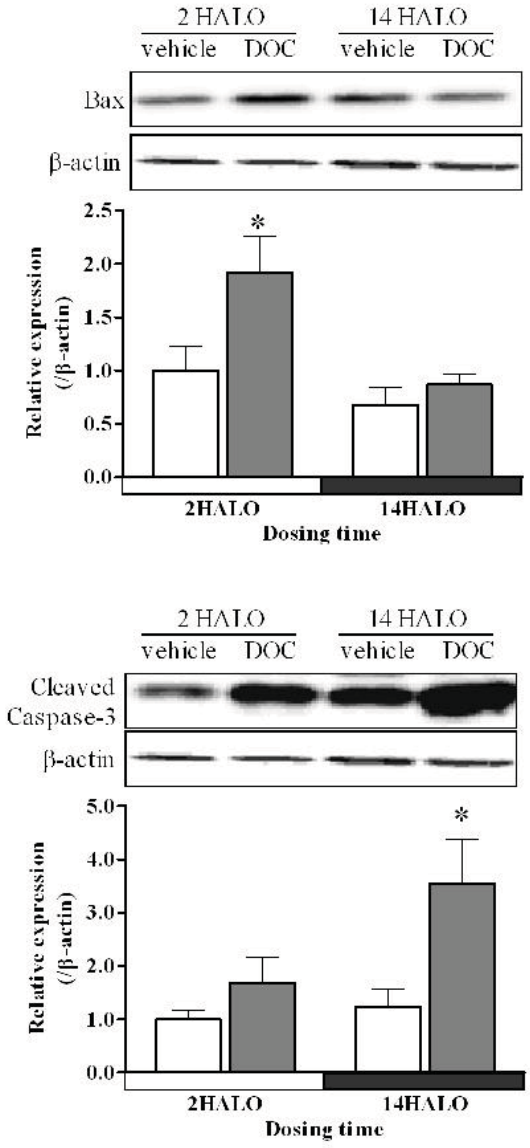

Fig. 2

JPET Fast Forward. Published on July 26, 2013 as DOI: 10.1124/jpet.113.203299
This article has not been copyedited and formatted. The final version may differ from this version.

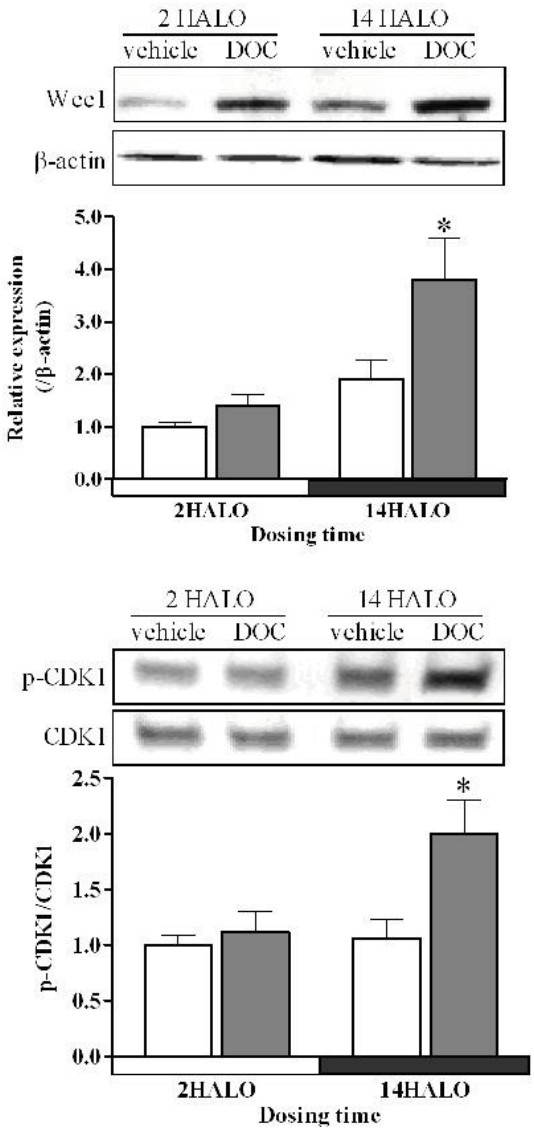

Fig. 3-1

JPET Fast Forward. Published on July 26, 2013 as DOI: 10.1124/jpet.113.203299
This article has not been copyedited and formatted. The final version may differ from this version.

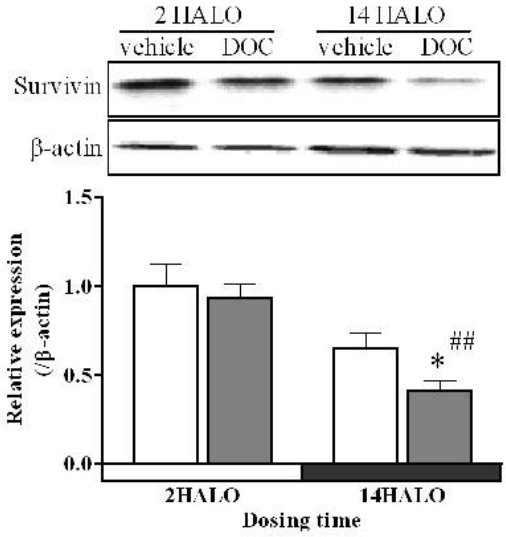

Fig. 3-2

JPET Fast Forward. Published on July 26, 2013 as DOI: 10.1124/jpet.113.203299
This article has not been copyedited and formatted. The final version may differ from this version.

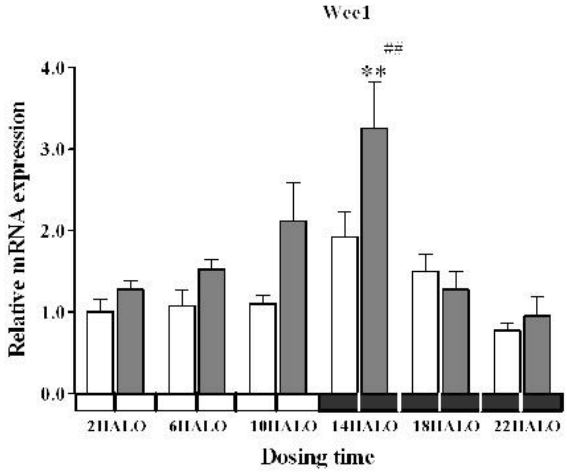

Fig. 4-1

JPET Fast Forward. Published on July 26, 2013 as DOI: 10.1124/jpet.113.203299
This article has not been copyedited and formatted. The final version may differ from this version.

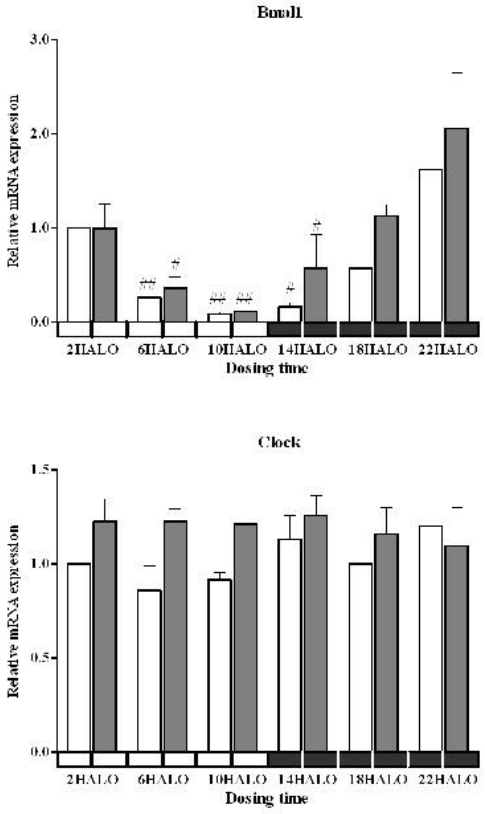

Fig. 4-2

JPET Fast Forward. Published on July 26, 2013 as DOI: 10.1124/jpet.113.203299
This article has not been copyedited and formatted. The final version may differ from this version.

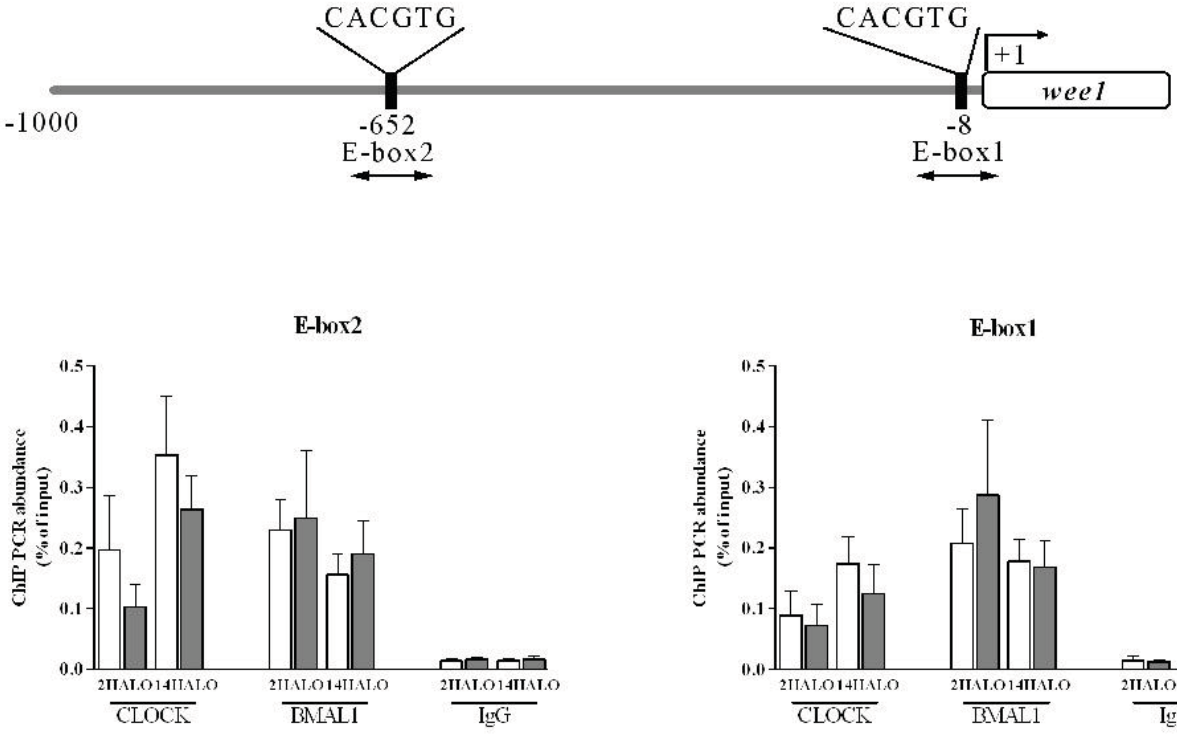

Fig. 5

JPET Fast Forward. Published on July 26, 2013 as DOI: 10.1124/jpet.113.203299
This article has not been copyedited and formatted. The final version may differ from this version.

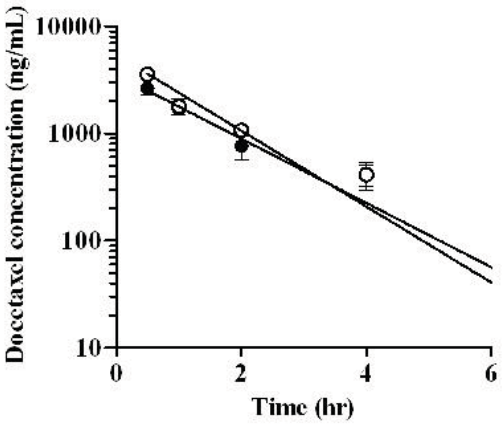

Fig. 6

JPET Fast Forward. Published on July 26, 2013 as DOI: 10.1124/jpet.113.203299
This article has not been copyedited and formatted. The final version may differ from this version.

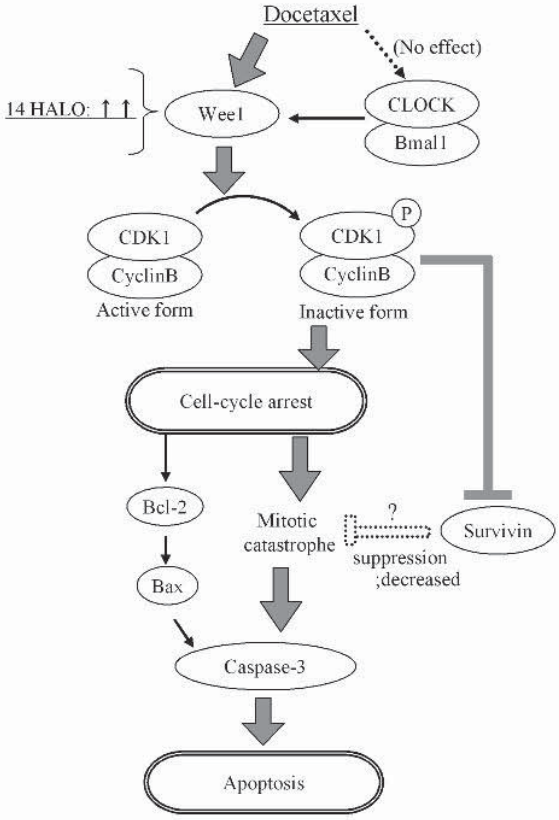

Fig. 7